Acta Oceanol. Sin., 2024, Vol. 43, No. 10, P. 100–106
https://doi.org/10.1007/s13131-024-2413-9
http://www.aosocean.com
E-mail: ocean2@hyxb.org.cn

Bioturbation coefficients and organic carbon degradation rates of deep-sea sediments in the central-eastern tropical Pacific

Feng Lin[1], Cai Lin[1]*, Xiuwu Sun[1], Hui Lin[1], Li Lin[1], Fangfang Deng[1], Kaiwen Tan[1], Peng Lin[2]

[1] Laboratory of Marine Ecological Environmental Early Warning and Monitoring, Third Institute of Oceanography, Xiamen 361005, China

[2] Savannah River Ecology Laboratory, University of Georgia, Aiken 29802, USA

Received 22 January 2024; accepted 23 May 2024

Abstract

The biogeochemical processes of marine sediments are influenced by bioturbation and organic carbon decomposition, which is crucial for understanding global element cycles and climate change. Two sediment cores were acquired in 2017 from abyssal basins in the central-eastern tropical Pacific to determine the bioturbation and organic carbon degradation processes. The radioactivity concentrations of ^{210}Pb and ^{226}Ra in the sediment cores were measured, indicating the presence of significant excess ^{210}Pb (^{210}Pb$_{ex}$) signals in the sediment cores. Besides, a manganese nodule was discovered in one core, which had a substantial influence on the distribution of ^{210}Pb$_{ex}$. With the exception of this anomalous finding, the bioturbation coefficients in the remaining core were estimated to be 10.6 cm^2/a using a steady-state diffusion model, greater than most of the deep-sea sediments from the equatorial eastern Pacific. By using a bio-diffusion model, we further calculated the degradation rates of organic carbon (8.02 ka^{-1}), which is also higher than other areas of the Pacific. Our findings displayed the presence of a biologically active benthic ecosystem in the central-eastern tropical Pacific.

Key words: ^{210}Pb, ^{226}Ra, bioturbation, tropical Pacific, organic carbon, degradation rate

Citation: Lin Feng, Lin Cai, Sun Xiuwu, Lin Hui, Lin Li, Deng Fangfang, Tan Kaiwen, Lin Peng. 2024. Bioturbation coefficients and organic carbon degradation rates of deep-sea sediments in the central-eastern tropical Pacific. Acta Oceanologica Sinica, 43(10): 100–106, doi: 10.1007/s13131-024-2413-9

1 Introduction

Several processes can substantially modify the biological, chemical, and physical properties of sediments, including bioturbation, organic remineralization, and physical sediment transport processes (Aller, 1994; Steiner et al., 2016; Wheatcroft et al., 1990), affecting early diagenesis in surface sediments and sedimentary record, as well as the structure and evolution of seafloor communities (Yang and Zhou, 2004). For example, bioturbation can transport freshly deposited materials to deep sediment and result in various biogeochemical consequences. Furthermore, the bioturbation-derived mixing of materials between different aged-sediments and degradation of organic matter would also decrease the temporal resolution from sedimentary records over a wide timescale (Song et al., 2022; Smith and Schafer, 1984). Therefore, a quantitative understanding of biological mixing (i.e., bioturbation) is essential in predicting the behavior of resettled substances from mining activities. Besides, majority of the deposited organic matter may be decomposed by the biological communities that reside within the shallow sediment depths, making the bioturbation playing an important role on organic matter degradation in different spatial and timescales (Banta et al., 1995). Bioturbation can enhance degradation rates of sedimentary organic matter by stimulating priming, i.e., the mixing of freshly deposited material into deeper sediment layers (Arndt et al., 2013; Kristensen et al., 2011), consequently further affecting the net CO_2 removal from the atmosphere.

The disequilibria between two naturally occurring radionuclides, radium-226 (^{226}Ra) and lead-210 (^{210}Pb) have been extensively used to examine the diagenetic processes and establish the timescales of sedimentation within the sediments (Yu et al., 2023; Nozaki et al., 1977; Soetaert et al., 1996; Suckow et al., 2001). Atmospherically derived ^{210}Pb (^{210}Pb$_{xs}$), produced from the decay of its parent nuclide, radon-222 (the daughter nuclide of ^{226}Ra), are delivered to the waters via fallout and rapidly adsorb to sediment particles, leading to a net excess of ^{210}Pb (^{210}Pb$_{ex}$) relative to ^{226}Ra that can be detectable for the sediment column deposited within 100 a if sediment accumulation alone controls the distribution of ^{210}Pb$_{ex}$. Nevertheless, the sediment mixing by bioturbation can cause the ^{210}Pb$_{ex}$ signal extending downward below the expected zero-activity depth of ocean sediments, which makes the ^{210}Pb-^{226}Ra disequilibria as a useful radiotracer pair to quantify the bioturbation-derived mixing depth (Suckow et al., 2001; Lin et al., 2021).

In the present study, two sediment cores were collected from the central-eastern tropical Pacific Ocean, followed by the application of the isotope pair ^{210}Pb-^{226}Ra to estimate the bioturbation coefficients (D_B) using a steady-state diffusion model. Additionally, D_B was further combined with the organic carbon to quantify the degradation rates of organic carbon by a bio-diffusion model to understand the bioturbation-derived dynamics of or-

Foundation item: The Scientific Research Foundation of Third Institute of Oceanography, Ministry of Natural Resources under contract No. 2020012; the Natural Science Foundation of Xiamen, China under contract No. 3502Z20227246; the Guiding Project of the Science and Technology Plan of Fujian Province under contract No. 2020Y0081.
*Corresponding author, E-mail: lincai@tio.org.cn

ganic carbon in deep Pacific sediments. Furthermore, the D_B in the study area was compared with that from other deep sea regions.

2 Materials and methods

2.1 *Sampling*

During the past decades, widespread deposition of manganese nodules onto the deep sediments of the Pacific and Indian oceans have received attention because of their potential as a valuable source of precious metals (Blöthe et al., 2015; Mukhopadhyay et al., 2019). The water column for tropical central-eastern Pacific Ocean region is mainly composed by six water masses, similar to those of polymetallic nodule exploration contract regions in the eastern Pacific and adjacent waters (Wang et al., 2013), including the Pacific Equatorial Water, North Pacific Central Water, California Central Water, South Pacific Central Water, Subarctic Pacific Water, and North Pacific Bottom Water, from top to bottom (Kuang et al., 2022).

During the R/V *Xiangyanghong 03* Cruise in autumn 2017, two sediment cores were collected in the central Pacific Ocean by a multiple-corer, which was utilized to gather sediments without disturbance (Fig. 1 and Table 1). Water depth in the study area ranges from 4 300 m to 6 450 m, with an average water depth of 5 350 m.

After collection, they were sliced into 1 cm intervals for the upper 2 cm and 2 cm slices for remaining core. Each subsample was sealed in a clean polyethylene box, and frozen at –18℃. The sediment samples were freeze-dried and homogenized before the analysis of water contents, total organic carbon (TOC) and two radionuclides (i.e., ^{210}Pb and ^{226}Ra). Water content was determined gravimetrically during freeze-drying.

Our sampling showed that surface sediment in the deep-sea basin area is clayey silt, and sand contents increases gradually from bottom to top. In the hilly region, the sediment type is clay silt, the content of sand is 1.33% to 21.2%, with an average of 11.11%. The change in sand and clay content is not obvious from bottom to top. The properties of the seafloor sediments do not change much, and they are mainly clay silty sand. The stratification of the sediments in the low and gentle hilly area is weaker than that in the deep basin area (Lin et al., 2022).

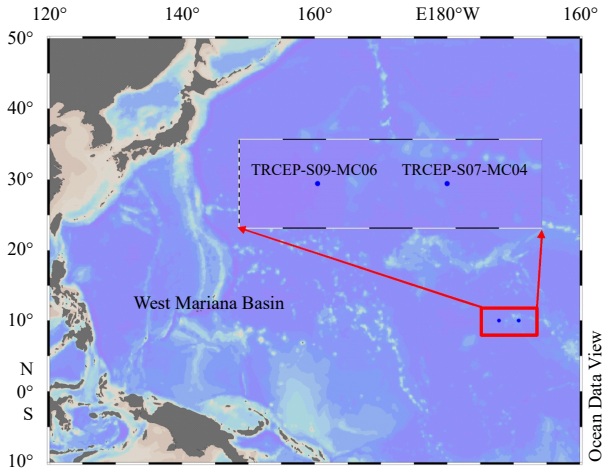

Fig. 1. Sampling locations in the central-eastern tropical Pacific.

2.2 *Measurement of total organic carbon*

The profile of TOC was determined in two sediment cores based on Guo and Macdonald (2006) with some modification. Briefly, an approximate 1 g sample was firstly acidified for 24 h with 4 mol/L HCl solution to remove the inorganic carbon, followed by a minimum of 3 deionized water rinses. Prior to measurement with a Fisons CHN elemental analyzer, the residues were dried at 50℃ and ground for homogenization. The subsamples were analyzed in duplicate to obtain the averaged values of TOC. The precision of the TOC analysis was ±0.01% as determined by replicate analysis of standards and samples.

2.3 *Determination of ^{210}Pb and ^{226}Ra in sediments*

The homogenized and dried samples of different sediment depths were placed into gamma counting tubes for the analysis by an ORTEC 9030 high-purity germanium well gamma detector at the decay energies of 46.5 keV for ^{210}Pb. The sediment samples were sealed for at least three weeks to allow secular equilibrium ingrowth of gaseous ^{222}Rn from the decay of ^{226}Ra, the parent nuclide of ^{210}Pb. Then the supported ^{210}Pb were determined from the activity of the ^{214}Bi from the ^{222}Rn, at the decay energy of 609.3 keV. The $^{210}Pb_{ex}$ in sediments were determined based on the difference between total activity of ^{210}Pb and the supported ^{210}Pb (Schmidt et al., 2021).

All samples were prepared with the same geometries and counted until a counting errors of <10% was obtained. Counting efficiencies were calibrated using the different masses (1–20 g) of marine sediment standard (IAEA-385). A correction for the self-absorption of the low-energy ^{210}Pb gamma rays was made using the method of Cutshall et al. (1983). Activities concentrations of ^{210}Pb will be decay-corrected to the date of collection.

2.4 *Models*

2.4.1 *Steady-state diffusion model*

In deep-sea sediments, potential bioturbation under the low sedimentation rates (usually 1–10 cm/ka) controls the penetration of $^{210}Pb_{ex}$ to a depth of several centimeters. Therefore, the sediment profile of $^{210}Pb_{ex}$ can be used to derive the mixing by bio-diffusion from the advection-diffusion equation (Díaz-Asencio et al., 2020). Assuming a steady-state diffusion model which includes radioactive decay to describe the process of bioturbation (Cullen, 1973; Guinasso and Schink, 1975) as:

$$\frac{\partial}{\partial x}\left(\rho D_B \frac{\partial A}{\partial x}\right) = \frac{\partial}{\partial t}(\rho A) + \frac{\partial}{\partial x}(\rho S A) + \lambda \rho A, \tag{1}$$

where D_B represents the bioturbation coefficient (cm^2/a), x represents the depth within the sediment column (cm), A represents the activity concentration of $^{210}Pb_{ex}$ (Bq/kg) in the depth of x, t represents the time (a), ρ represents the bulk sediment density (g/cm^3), S represents the sedimentation rate (cm/a) and λ represents the decay constant of ^{210}Pb (0.031 a^{-1}).

Table 1. Sampling locations, water depth, bioturbation (D_B), mixing depth (L), and organic carbon degradation (OCD)

Station	Latitude	Longitude	Depth/m	D_B/(cm^2·a^{-1})	L/cm	OCD/ka^{-1}
TRCEP-S09-MC06	9.998 8°N	172.196 8°W	5 721	10.6	18.5	8.02
TRCEP-S07-MC04	10.000 5°N	169.199 6°W	4 797	–	–	–

Note: – represents no data.

DeMaster and Cochran (1982) derived an equation that approximates D_B, assuming that in the mixing layer, D_B, S, and ρ are in a constant state.

The solution with the boundary conditions, assuming that $A = A_0$ for $x = 0$ and $A \to 0$ for $x \to \infty$, Eq. (1) is solved analytically, resulting in as following:

$$A = A_0 \exp\left[\frac{S - \sqrt{S^2 + 4\lambda D_B}}{2D_B} x\right]. \quad (2)$$

Since the deposition rate of deep sea is generally low (1–10 mm/ka), and the timescale of the ^{210}Pb-derived bioturbation is only about 100 a, the deposition of sediments can be ignored within the timescale of the tracer.

$$D_B = \frac{\lambda x^2}{\ln(A_0/A)}. \quad (3)$$

2.4.2 *Bio-diffusion model*

Organic matter can be transported to deeper sediment layer by bioturbation. Assuming the bulk density and sedimentation rate are constant (Canfield, 1994; Yang and Zhou, 2004), based on one-dimensional, we can use profiles of $^{210}Pb_{ex}$ and its relationship with TOC to derive an equation as:

$$D_B \frac{\partial^2 F_m}{\partial x^2} = S \frac{\partial F_m}{\partial x} + kF_m, \quad (4)$$

where F_m denotes the metabolizable organic carbon, and k represents degradation rate of organic carbon (ka^{-1}). According to the boundary conditions: $F_m = F_{m0}$ at $x = 0$, and $F_m \to 0$ at $x \to \infty$, the F_m can be obtained as:

$$F_m = F_{m0} e^{-\frac{-S + \sqrt{S^2 + 4D_B k}}{2D_B} x}. \quad (5)$$

Based on the mass balance, the TOC can be further described as:

$$F_t = F_{m0} e^{-\frac{-S + \sqrt{S^2 + 4D_B k}}{2D_B} x} + F_{nm}, \quad (6)$$

where F_{nm} is non-metabolizable organic carbon.

3 Results and discussion

3.1 *TOC and water content*

The sediment profiles of the TOC concentrations were presented in Fig. 2. The results showed an evident decreasing trend of TOC contents with increasing sediment depth. TOC contents in the core TRCEP-S09-MC06 ranged from 0.23% to 0.42%, averaging 0.32% ± 0.07%, high than those in seamounts of the northwestern tropical Northwest Pacific (0.14%–0.28%, Lin et al., 2021). In comparison, TOC contents in the core TRCEP-S07-MC04 were lower than TRCEP-S09-MC06, ranging from 0.18% to 0.26% with an average concentration of 0.21% ± 0.04%. Similar to the TOC, TRCEP-S09-MC06 core also showed higher water content than that in TRCEP-S07-MC04 core in general, with a decreasing from 89% to 78% with depth in TRCEP-S09-MC06 core and 79% to 60% in TRCEP-S07-MC04, respectively. Together, we can safely suggest that our two sampling stations may have different depositional environments in central-eastern tropical Pacific Ocean.

3.2 *Profiles of ^{226}Ra and ^{210}Pb*

The distribution of ^{226}Ra and ^{210}Pb in two sediment cores are shown in Fig. 3. ^{226}Ra values varied from 130 Bq/kg to 298 Bq/kg with the highest value at the 15 cm of TRCEP-S09-MC06. For the

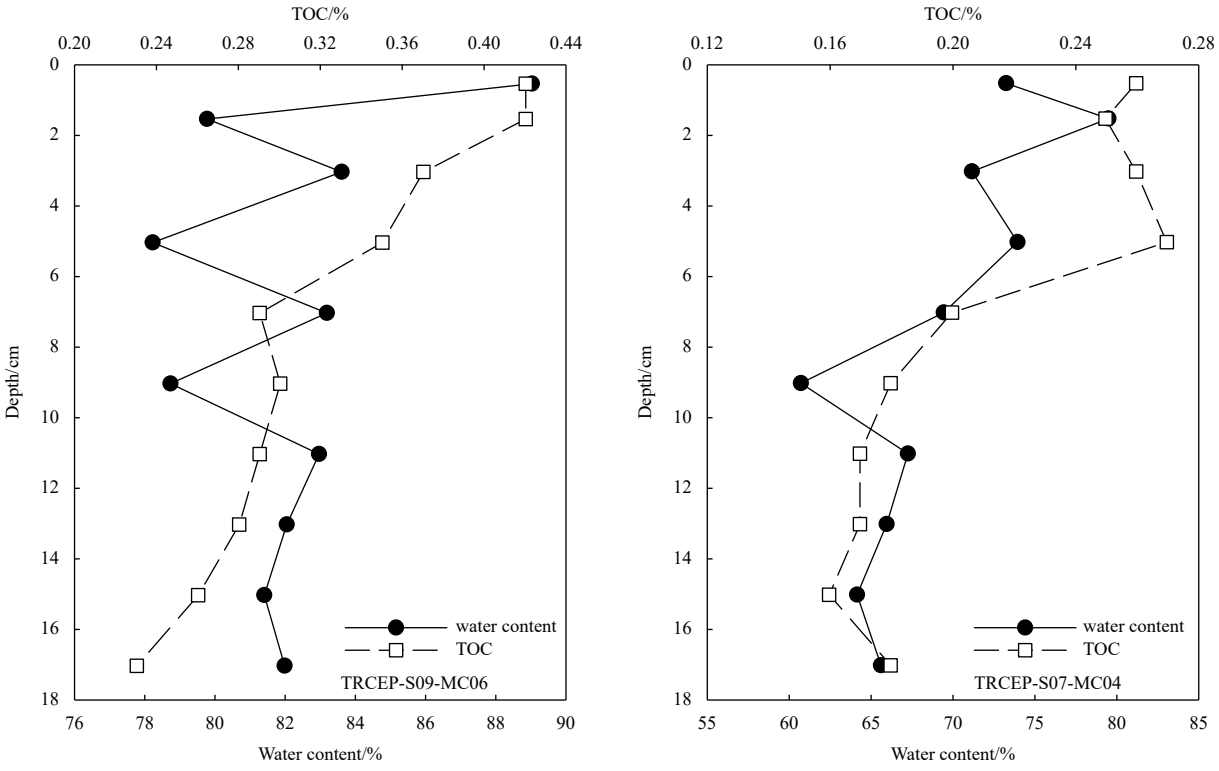

Fig. 2. Profiles of TOC and water content in two sediment cores. The dots represent the water content, and the square represents the TOC.

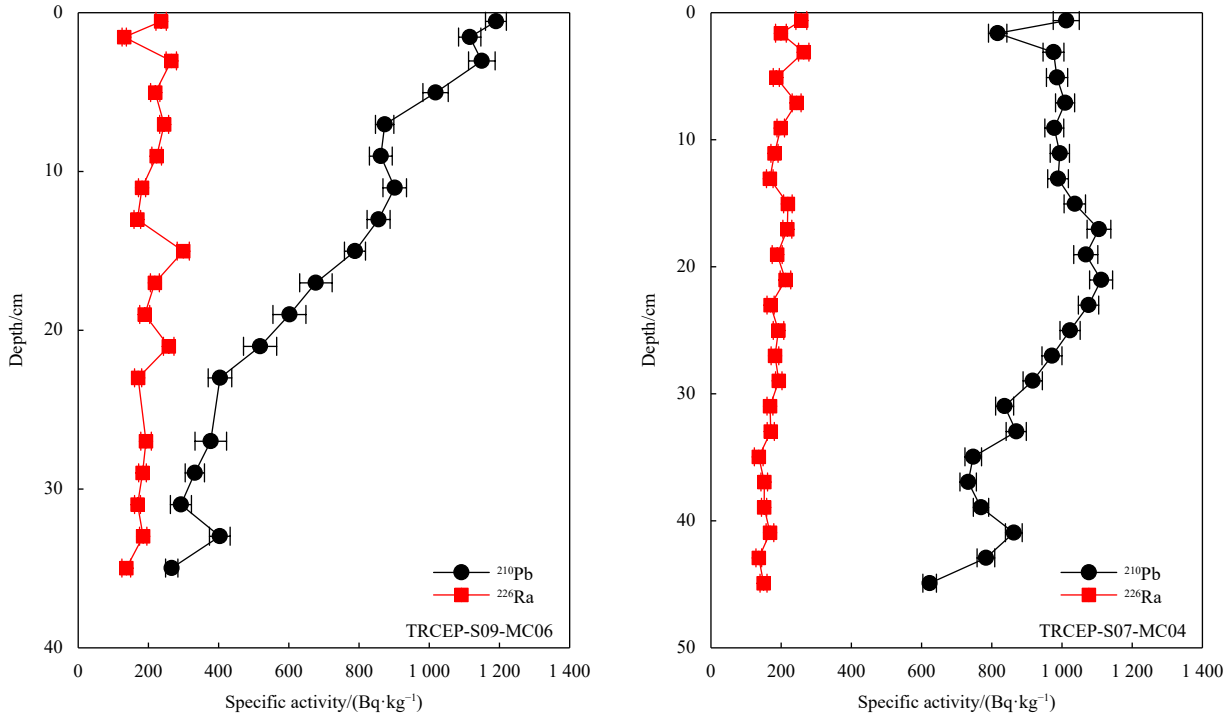

Fig. 3. Profiles of specific activity of ^{210}Pb and ^{226}Ra in two sediment cores.

TRCEP-S07-MC04, the highest value of ^{226}Ra was observed at 3 cm. As shown in Fig. 3, there will be not an evident change with depth for both ^{226}Ra profiles.

The ^{210}Pb in the sediment cores ranged from 266 Bq/kg to 1 190 Bq/kg, with an average of (832 ± 251) Bq/kg. The specific activity concentrations of ^{210}Pb in TRCEP-S09-MC06 core consistently decreased gradually with depth, similar to the observation all throughout the ocean (Lin et al., 2021; Steiner et al., 2016; Yang et al., 2020). In contrast, increasing ^{210}Pb was observed between 16 cm and 21 cm of TRCEP-S07-MC04 core with the highest value at 21 cm, followed by a rapid decrease in the deeper sediment column (>21 cm). Such $^{210}Pb_{ex}$ variation trends, especially in TRCEP-S07-MC04 core may be a strong indicator showing the presence of bioturbation processes which introduced the freshly deposited sediments into the deeper sediment column, similar to previous observations in other oceans basins. For example, the secondary high value of ^{210}Pb in the sediments collected from the Peru Basin appeared at the depth of 5–20 cm, which was believed to be caused by subsurface excretion and surface feeding of animals such as echinacea (Suckow et al., 2001). The Tropical Pacific Ocean sediments showed the ^{210}Pb peak at subsurface sediments between 22–28 cm and 6–10 cm, attributed to Yi insect and rotate the trail of *in-situ* hybrid (Yang and Zhou, 2004).

The vertical distribution and highest value of the specific activity of ^{210}Pb were significantly different in deep-sea sediments at different stations, indicating that the deposition of ^{210}Pb onto the sediments was location-dependent (Suckow et al., 2001; Yang et al., 2020). In different sediment cores collected in the western North Pacific and the same stations in the eastern equatorial Pacific, there were significant differences in specific activity and preservation of ^{210}Pb (Thiel and Tiefsee-Umweltschutz, 2001; Yang et al., 2020). These observations show that the settlement of the deep sea sediments is spatially inhomogeneous.

Additionally, at 20 cm of the TRCEP-S07-MC04 core, a hidden manganese nodule was discovered, with a diameter of approximately 1.5 cm (Fig. 4). The specific activity of ^{226}Ra in the manganese nodule is 2 150 Bq/kg (this value was also measured by our gamma detector), similar to the observation reported by Suckow et al. (2001). The buried manganese nodule can be a source of ^{222}Rn produced by the decay of ^{226}Ra, consequently serving as the potential source for ^{210}Pb (Cochran and Krishnaswami, 1980). The molecular diffusion constant of radon in sediment is 1.2×10^{-5} cm^2/s (Martens et al., 1980), 1–2 orders of magnitude higher than the global mean value of bioturbation

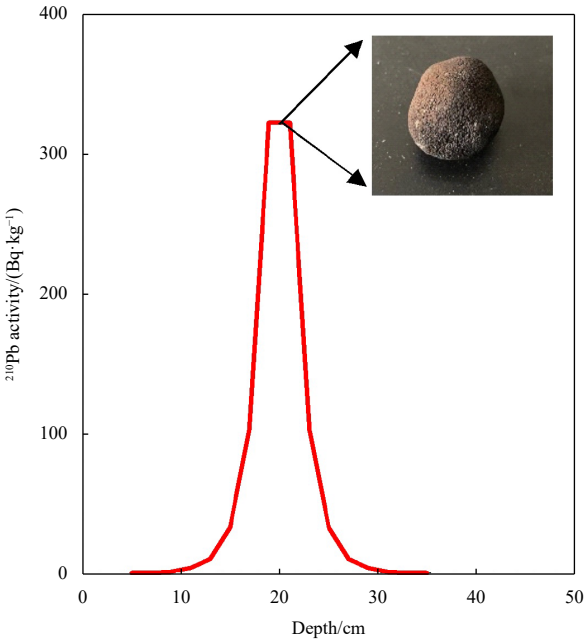

Fig. 4. The curve of ^{210}Pb activity from the one-dimensional diffusion module of ^{222}Rn which is escaped from manganese nodule (sediment core TRCEP-S07-MC04).

coefficient (19.98 ± 42.64) cm^2/a (Teal et al., 2008). Due to the short half-life of ^{222}Rn (3.8 d) compared with ^{210}Pb, assuming the escape factor for ^{222}Rn is 15% of the activity of ^{226}Ra measured within the nodule (Suckow et al., 2001), the high value of ^{210}Pb in the subsurface sediment observed in the present study (Fig. 3) may be partially affected by the manganese nodule discovered in the TRCEP-S07-MC04 core. The inventory of ^{210}Pb from the influence of the manganese nodule was estimated to be about 20% of the total ^{210}Pb pool at the depth of 19 cm and 21 cm.

3.3 *Vertical distribution of $^{210}Pb_{ex}$*

The specific activity of $^{210}Pb_{ex}$ in the cores ranged from 123 Bq/kg to 984 Bq/kg, with an average of (636 ± 242) Bq/kg. In the TRCEP-S09-MC06 core, the $^{210}Pb_{ex}$ gradually decreases with increasing depth (Fig. 5). In contrast, in the TRCEP-S07-MC04 core, the $^{210}Pb_{ex}$ increased gradually with the depth between surface and 23 cm and then decreased gradually with sediment depth.

Similar observation showing a maximum of $^{210}Pb_{ex}$ at subsurface (5–20 cm), without any indication of elevated ^{226}Ra was also reported in other ocean regions (Smith et al., 1986; Suckow et al., 2001; Yang et al., 2020). A hybrid model "conveyor belt" or "none-*in-situ* mixing" was proposed to be responsible for the observed maximum value in subsurface sediments, i.e., organic matter and radionuclide-enriched surface sediments consumed by the benthos were excreted to the subsurface sediments (Smith et al., 1986). In regard to this study, as ^{210}Pb has a half-life of 22.3 a, the $^{210}Pb_{ex}$ signal can be only detectable within roughly 100 a. Considering the very low sedimentation rates (few millimeters per thousand years) in the study area, the observed $^{210}Pb_{ex}$ variation trend and signals as shown in Fig. 5, therefore, can strongly indicate the occurrence of bioturbation in the sediments. Nevertheless, the $^{210}Pb_{ex}$ signal can be also attributed to the possibility that ^{226}Ra diffusing into deep sediments through pore water and being trapped in manganese-enriched layers (Díaz-Asencio et al., 2020; Suckow et al., 2001), like our discovered manganese nodule at 20 cm of the TRCEP-S07-MC04 core (Fig. 4). Unfortunately, the ^{210}Pb supported by manganese nodule-derived ^{226}Ra cannot be quantified in the present study due to difficulties determining if other manganese nodules were present in the surrounding area of the sampling location, which requires further study in future.

3.4 *Bioturbation coefficient*

While evaluating the bioturbation coefficient, the possibility of $^{210}Pb_{ex}$ being impacted by non-local mixing and manganese nodules cannot be ignored. Due to the uncertainty of the ^{210}Pb possibly supported by the manganese nodule in TRCEP-S07-MC04 core, only TRCEP-S09-MC06 was included in the D_B estimation, which was calculated based on the sediment profile of $^{210}Pb_{ex}$.

According to the decreasing trend of $^{210}Pb_{ex}$ in Fig. 5, the D_B and L at station TRCEP-S09-MC06 were estimated to be 10.6 cm^2/a and 18.5 cm, respectively. This was significantly lower than the D_B of seamounts in the northwestern tropical Pacific (16.8 and 24.1 cm^2/a, Lin et al., 2021; 27.1 cm^2/a, Yang et al., 2020). Though, it was higher than the estimated D_B values in deep-sea sediments of the equatorial eastern Pacific (Hyeong et al., 2018), the northeast tropical Pacific, the equatorial Pacific and the western Pacific (Alperin et al., 2002; Hyeong et al., 2018; Smith et al., 1997, 1998; Yang and Zhou, 2004; Yang et al., 2011) (Table 2). This demonstrated that the study area, central-eastern tropical Pacific, had greater benthic biological activity than other regions of the Pacific Ocean.

Several previous studies have demonstrated that the positive correlation between the organic carbon concentration and the bioturbation intensity (Lin et al., 2021; Yang and Zhou, 2004; Yang et al., 2011). However, an opposite trend was found when comparing different regions of Pacific Ocean according to the data summarized in Table 2, showing high D_B corresponding with lower TOC. Increased food supply may lower bioturbation intensity since deposit feeders may reduce sediment reprocessing rates at times of high food availability due to homeostatic feeding (Jumars and Wheatcroft, 1989). Cammen (1979) demonstrated that the rate of ingestion varies inversely with the proportion of organic carbon in accessible sediments.

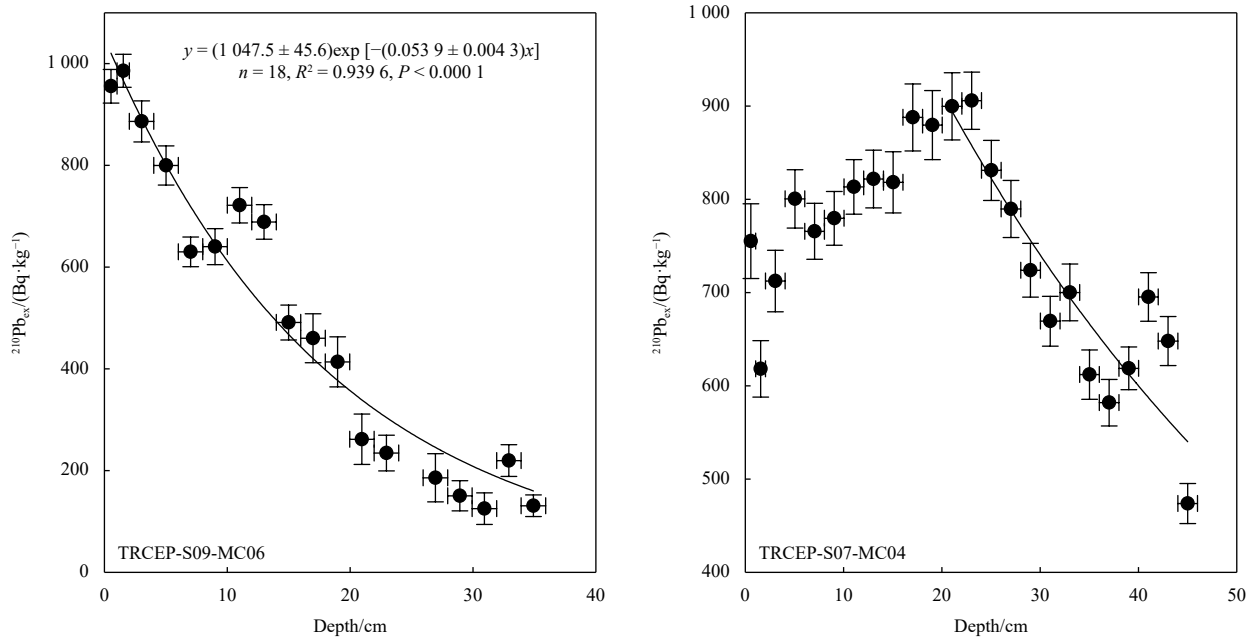

Fig. 5. The relationship between the specific activity of $^{210}Pb_{ex}$ (Bq/kg) and depth (cm) in two sediment cores.

Table 2. ^{210}Pb-derived bioturbation coefficients (D_B) in the Pacific Ocean

Research area	D_B/(cm^2·a^{-1})	TOC/%	References
Northwest tropical Pacific	16.8–24.1	0.19	Lin et al., 2021
Northwest Pacific	1.01–27.1	0.26	Yang et al., 2020
Equatorial eastern Pacific	1.1–9.0	0.5	Hyeong et al., 2018
Northeast Pacific	2.1–4.4		Smith et al., 1998
Northeast tropical Pacific	0.26–2.75	0.33	Yang and Zhou, 2004
Equatorial Pacific	0.02–1.0		Smith et al., 1997
Western Pacific	1.59–8.64	0.47	Yang et al., 2011
Central-eastern tropical Pacific	10.6	0.32	this study

Inversely, Middelburg et al. (1997) proposed an empirical to the relationship between the bioturbation coefficient and water depth based on data from the eastern Pacific and the North Atlantic. According to the equation ($D_B = 5.2 \times 10^{0.762-0.004Z}$), the D_B in this study area is estimated to be 0.15 cm^2/a and 0.36 cm^2/a, which is two orders of magnitude lower than those derived by ^{210}Pb$_{ex}$ (Table 2). It should be mentioned that the statistical relationship between bioturbation coefficient and water depth were based on global sediment bioturbation data, which may not account for specific regional characteristics. More characteristics are required for a comparison between regions, such as bottom current, oxygen penetration into sediment, sedimentation rate, organic carbon concentration in surface sediment, and burial flow of particulate organic carbon at the sediment-water interface.

3.5 *Degradation of organic carbon*

Based on the reported sedimentation rate of 0.5 mm/ka in the study area (Müller and Mangini, 1980) and our observed D_B of 10.6 cm^2/a, we can calculate organic carbon degradation rates using the Eq. (5) above. As shown in Fig. 6, the degradation rate of metabolizable organic carbon was estimated to be 8.02 ka^{-1}, higher than those in the central Pacific, Northeast Pacific, and central North Pacific (0.003 2–4.97 ka^{-1}) (Müller and Mangini, 1980; Murray and Kuivila, 1990), suggesting that the recycling of organic matter in the sediment of central-eastern tropical Pacific Ocean was stronger than some other regions of Pacific Ocean.

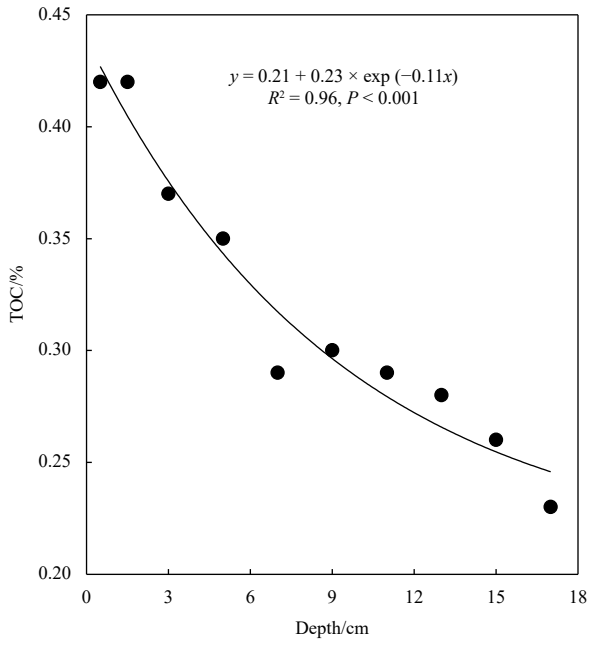

Fig. 6. The content of TOC varies with depth.

4 Conclusions

In the central-eastern tropical Pacific, radionuclide activities of ^{210}Pb and ^{226}Ra were measured in the sediment cores. Significant ^{210}Pb$_{ex}$ signals were found in both sediment cores. Based on the one-dimensional steady-state vortex diffusion model, the bioturbation coefficient of sediments was calculated (10.6 cm^2/a) after removing the core impacted by the ^{210}Pb signal from the manganese nodule. This is lower than the global average but higher than many deep sea areas. By using a bio-diffusion model, the degradation rates of organic carbon (8.02 ka^{-1}) were calculated, which were higher than most of the Pacific. This indicated the study area has a more biological active benthic ecosystem than most deep basin areas.

Acknowledgements

We gratefully acknowledge Nicholas Wellbrock from Texas A&M University Galveston Campus for his assistance on the manuscript editing.

References

Aller R C. 1994. Bioturbation and remineralization of sedimentary organic matter: Effects of redox oscillation. Chemical Geology, 114(3–4): 331–345, doi: 10.1016/0009-2541(94)90062-0

Alperin M J, Suayah I B, Benninger L K, et al. 2002. Modern organic carbon burial fluxes, recent sedimentation rates, and particle mixing rates from the upper continental slope near Cape Hatteras, North Carolina (USA). Deep-Sea Research Part II: Topical Studies in Oceanography, 49(20): 4645–4665, doi: 10.1016/S0967-0645(02)00133-9

Arndt S, Jørgensen B B, LaRowe D E, et al. 2013. Quantifying the degradation of organic matter in marine sediments: A review and synthesis. Earth-Science Reviews, 123: 53–86, doi: 10.1016/j.earscirev.2013.02.008

Banta G T, Giblin A E, Hobbie J E, et al. 1995. Benthic respiration and nitrogen release in Buzzards Bay, Massachusetts. Journal of Marine Research, 53(1): 107–135, doi: 10.1357/0022240953213287

Blöthe M, Wegorzewski A, Müller C, et al. 2015. Manganese-cycling microbial communities inside deep-sea manganese nodules. Environmental Science & Technology, 49(13): 7692–7700

Cammen L M. 1979. Ingestion rate: An empirical model for aquatic deposit feeders and detritivores. Oecologia, 44(3): 303–310, doi: 10.1007/BF00545232

Canfield D E. 1994. Factors influencing organic carbon preservation in marine sediments. Chemical Geology, 114(3–4): 315–329, doi: 10.1016/0009-2541(94)90061-2

Cochran J K, Krishnaswami S. 1980. Radium, thorium, uranium, and ^{210}Pb in deep-sea sediments and sediment pore waters from the North Equatorial Pacific. American Journal of Science, 280(9): 849–889, doi: 10.2475/ajs.280.9.849

Cullen D J. 1973. Bioturbation of superficial marine sediments by interstitial meiobenthos. Nature, 242(5396): 323–324, doi: 10.1038/242323a0

Cutshall N H, Larsen I L, Olsen C R. 1983. Direct analysis of ^{210}Pb in sediment samples: Self-absorption corrections. Nuclear Instru-

ments and Methods in Physics Research, 206(1–2): 309–312, doi: 10.1016/0167-5087(83)91273-5
DeMaster D J, Cochran J K. 1982. Particle mixing rates in deep-sea sediments determined from excess 210Pb and 32Si profiles. Earth & Planetary Science Letters, 61(2): 257–271
Díaz-Asencio M, Herguera J C, Schwing P T, et al. 2020. Sediment accumulation rates and vertical mixing of deep-sea sediments derived from ^{14}C and ^{210}Pb in the southern Gulf of Mexico. Marine Geology, 429: 106288, doi: 10.1016/j.margeo.2020.106288
Guinasso N L Jr, Schink D R. 1975. Quantitative estimates of biological mixing rates in abyssal sediments. Journal of Geophysical Research, 80(21): 3032–3043, doi: 10.1029/JC080i021p03032
Guo Laodong, Macdonald R W. 2006. Source and transport of terrigenous organic matter in the upper Yukon River: Evidence from isotope ($\delta^{13}C$, $\Delta^{14}C$, and $\delta^{15}N$) composition of dissolved, colloidal, and particulate phases. Global Biogeochemical Cycles, 20(2): GB2011
Hyeong K, Seo I, Lee H B, et al. 2018. Variability in particle mixing rates in sediments with polymetallic nodules in the equatorial eastern Pacific as determined from measurements of excess ^{210}Pb. Ocean Science Journal, 53(2): 355–368, doi: 10.1007/s12601-018-0026-y
Jumars P A, Wheatcroft R A. 1989. Responses of benthos to changing food quality and quanitity, with a focus on deposit feeding and bioturbation. In: Berger W H, Smetacek V S, Wefer G, eds. Productivity of the Ocean: Present and Past. New York: John Wiley Sons Press, 235–253
Kristensen E, Hansen T, Delefosse M, et al. 2011. Contrasting effects of the polychaetes *Marenzelleria viridis* and *Nereis diversicolor* on benthic metabolism and solute transport in sandy coastal sediment. Marine Ecology Progress Series, 425: 125–139, doi: 10.3354/meps09007
Kuang Fangfang, Cha Jing, Zhang Junpeng, et al. 2022. Intra-seasonal variability of the abyssal currents in COMRA's contract area in the Clarion-Clipperton Zone. Acta Oceanologica Sinica, 41(11): 1–11, doi: 10.1007/s13131-021-1945-5
Lin Feng, Lin Cai, Lin Hui, et al. 2021. ^{210}Pb-Derived bioturbation rates in sediments around seamounts in the tropical Northwest Pacific. Frontiers in Marine Science, 8: 701897, doi: 10.3389/fmars.2021.701897
Lin Cai, Liu Yang, Jiang Ronggen, et al. 2022. Baseline establishment for metals in the western Clarion-Clipperton Zone. Acta Oceanologica Sinica, 41(11): 12–22, doi: 10.1007/s13131-021-1908-x
Martens C S, Kipphut G W, Klump J V. 1980. Sediment-water chemical exchange in the coastal zone traced by *in situ* Radon-222 flux measurements. Science, 208(4441): 285–288, doi: 10.1126/science.208.4441.285
Middelburg J J, Soetaert K, Herman P M. 1997. Empirical relationships for use in global diagenetic models. Deep Sea Research Part I: Oceanographic Research Papers, 44(2): 327–344
Mukhopadhyay R, Naik S, De Souza S, et al. 2019. The economics of mining seabed manganese nodules: A case study of the Indian Ocean nodule field. Marine Georesources & Geotechnology, 37(7): 845–851
Murray J W, Kuivila K M. 1990. Organic matter diagenesis in the northeast Pacific: transition from aerobic red clay to suboxic hemipelagic sediments. Deep-Sea Research Part A: Oceanographic Research Papers, 37(1): 59–80
Müller P J, Mangini A. 1980. Organic carbon decomposition rates in sediments of the Pacific manganese nodule belt dated by ^{230}Th and ^{231}Pa. Earth and Planetary Science Letters, 51(1): 94–114, doi: 10.1016/0012-821X(80)90259-9
Nozaki Y, Cochran J K, Turekian K K, et al. 1977. Radiocarbon and ^{210}Pb distribution in submersible-taken deep-sea cores from Project FAMOUS. Earth and Planetary Science Letters, 34(2): 167–173, doi: 10.1016/0012-821X(77)90001-2
Schmidt N, Dellapenna T, Lin Peng. 2021. $^{7}Be/^{210}Pb_{xs}$ ratio-derived age and residence time of suspended sediments in Galveston Bay. Frontiers in Marine Science, 8: 703945, doi: 10.3389/fmars.2021.703945
Smith C R, Berelson W, Demaster D J, et al. 1997. Latitudinal variations in benthic processes in the abyssal equatorial Pacific: control by biogenic particle flux. Deep-Sea Research Part II: Topical Studies in Oceanography, 44(9–10): 2295–2317, doi: 10.1016/S0967-0645(97)00022-2
Smith J N, Boudreau B P, Noshkin V. 1986. Plutonium and ^{210}Pb distributions in northeast Atlantic sediments: subsurface anomalies caused by non-local mixing. Earth and Planetary Science Letters, 81(1): 15–28, doi: 10.1016/0012-821X(86)90097-X
Smith C R, Maybaum H L, Baco A R, et al. 1998. Sediment community structure around a whale skeleton in the deep Northeast Pacific: Macrofaunal, microbial and bioturbation effects. Deep-Sea Research Part II: Topical Studies in Oceanography, 45(1–3): 335–364, doi: 10.1016/S0967-0645(97)00043-X
Smith J N, Schafer C T. 1984. Bioturbation processes in continental slope and rise sediments delineated by Pb–210, microfossil and textural indicators. Journal of Marine Research, 42(4): 1117–1145, doi: 10.1357/002224084788520738
Soetaert K, Herman P M J, Middelburg J J, et al. 1996. Modeling ^{210}Pb-derived mixing activity in ocean margin sediments: Diffusive versus nonlocal mixing. Journal of Marine Research, 54(6): 1207–1227, doi: 10.1357/0022240963213808
Song Shasha, Santos I R, Yu Huaming, et al. 2022. A global assessment of the mixed layer in coastal sediments and implications for carbon storage. Nature Communications, 13: 4903, doi: 10.1038/s41467-022-32650-0
Steiner Z, Lazar B, Levi S, et al. 2016. The effect of bioturbation in pelagic sediments: Lessons from radioactive tracers and planktonic foraminifera in the Gulf of Aqaba, Red Sea. Geochimica et Cosmochimica Acta, 194: 139–152, doi: 10.1016/j.gca.2016.08.037
Suckow A, Treppke U, Wiedicke M H, et al. 2001. Bioturbation coefficients of deep-sea sediments from the Peru Basin determined by gamma spectrometry of $^{210}Pb_{exc}$. Deep-Sea Research Part II: Topical Studies in Oceanography, 48(17–18): 3569–3592, doi: 10.1016/S0967-0645(01)00057-1
Teal L, Bulling M T, Parker E, et al. 2008. Global patterns of bioturbation intensity and mixed depth of marine soft sediments. Aquatic Biology, 2(3): 207–218, doi: 10.3354/ab00052
Thiel H, Tiefsee-Umweltschutz F. 2001. Evaluation of the environmental consequences of polymetallic nodule mining based on the results of the TUSCH Research Association. Deep-Sea Research Part II: Topical Studies in Oceanography, 48(17–18): 3433–3452, doi: 10.1016/S0967-0645(01)00051-0
Wang Fan, Li Yuanlong, Zhang Yanhui, et al. 2013. The subsurface water in the North Pacific tropical gyre. Deep-Sea Research Part I: Oceanographic Research Papers, 75: 78–92, doi: 10.1016/j.dsr.2013.01.002
Wheatcroft R A, Jumars P A, Smith C R, et al. 1990. A mechanistic view of the particulate biodiffusion coefficient: step lengths, rest periods and transport directions. Journal of Marine Research, 48(1): 177–207, doi: 10.1357/002224090784984560
Yang Zifei, Qian Qiankun, Chen Min, et al. 2020. Enhanced but highly variable bioturbation around seamounts in the northwest Pacific. Deep-Sea Research Part I: Oceanographic Research Papers, 156: 103190, doi: 10.1016/j.dsr.2019.103190
Yang Weifeng, Zhang Xinxing, Chen Min, et al. 2011. Bioturbation in the western Pacific Ocean: use of ^{210}Pb to evaluate intensity and POC transport. Journal of Central South University: Science and Technology (in Chinese), 42(S2): 189–195
Yang Qunhui, Zhou Huaiyang. 2004. Bioturbation in near-surface sediments from the COMRA Polymetallic Nodule Area: evidence from excess ^{210}Pb measurements. Chinese Science Bulletin, 49(23): 2538–2542
Yu Wen, Lin Feng, Lin Longshan. 2023. Bioturbation in sediment cores from the Clarion-Clipperton Zone in the northeast Pacific: Evidence from excess ^{210}Pb. Marine Pollution Bulletin, 188: 114635, doi: 10.1016/j.marpolbul.2023.114635